Emergent, Collective Oscillations of Self-Mobile Particles and Patterned Surfaces under Redox Conditions

Michael E. Ibele,[†] Paul E. Lammert,[‡] Vincent H. Crespi,[‡,*] and Ayusman Sen[†,*]

[†]Department of Chemistry and [‡]Department of Physics, The Pennsylvania State University, University Park, Pennsylvania 16802

ABSTRACT We have discovered that silver chloride (AgCl) particles in the presence of UV light and dilute hydrogen peroxide exhibit both single-particle and collective oscillations in their motion which arise due to an oscillatory, reversible conversion of AgCl to silver metal at the particle surface. This system exhibits several of the hallmarks of nonlinear oscillatory reactions, including bistability, reaction waves, and synchronized collective oscillations at high particle concentrations. However, unlike traditional oscillatory reactions that take place among dispersed solute species in solution or near a fixed electrode surface, this system of self-mobile catalytic particles evinces a new dynamical length scale: the interparticle spacing, which appears to control wave propagation. The collective motions of these powered nanoparticles self-organize into clumped oscillators with significant spatiotemporal correlations between clumps. A variant of this system using a regular array of lithographically patterned silver disks supports the propagation of binary "On/Off" Ag/AgCl waves through the lattice.

KEYWORDS: colloids · oscillating reaction · nanomotor · collective behavior · catalysis

The "chemical clocks" in oscillating chemical reactions provide an archetypal example of emergent behavior in a system driven far from equilibrium.[1−4] Since their discovery by Fechner in the early 19th century,[1] oscillating chemical systems have been implicated in such diverse fields as biological morphogenesis,[5,6] neuron communication,[7] and the fabrication of artificial memory devices.[8] The well-known Belousov−Zhabotinsky (BZ) reaction, for example, produces periodic color changes in solution as a metal catalyst alternates between oxidation states.[9−12] BZ oscillations have also been observed in heterogeneous catalysis by incorporating the BZ catalyst into thermo-responsive hydrogels[13−15] or ion exchange beads.[16,17] The relevant dynamical degrees of freedom in these systems are continuum scalar fields: the local reactant concentrations. Here, we extend these phenomena to systems where the fundamental interacting degrees of freedom are not continuum fields but discretized mobile particles, and thereby couple the rich nonlinear dynamics of autocatalytic reactions to the collective motions of self-motile particles.[18−23] Further development of this concept may facilitate the design of novel reconfigurable materials.

We report the first example of synchronized oscillatory movement of colloidal silver chloride (AgCl) particles driven by a previously unknown chemical oscillating system in which AgCl is reversibly converted to silver metal in dilute aqueous solutions of hydrogen peroxide (H_2O_2) under UV irradiation. The underlying oscillatory reaction couples to particle motion by means of a diffusiophoretic interaction between the particles, an interaction which is generated by the ion gradients that build up around each particle as the reaction proceeds on their surface. Overlapping gradients between nearby particles drive a rich collective behavior.

RESULTS AND DISCUSSION

Oscillation of Silver Chloride Particles. In the initial experiment, AgCl particles of ~2 μm diameter were placed in dilute (~1% (v/V)) room temperature solutions of H_2O_2 on a microscope slide and illuminated from below with 320−380 nm UV light at 2.5 W cm^{-2}, focused by a 50× microscope objective. The particles were also backlit from above with low intensity (6 mW cm^{-2}) broad-spectrum visible light for imaging purposes. In the absence of UV, fresh AgCl particles settle to the slide surface and undergo simple Brownian motion in the plane of the slide. However, upon irradiation with UV light, the particles exhibit a distinctive oscillatory stick−slip motion: alternating between sticking to the underlying glass

*Address correspondence to asen@psu.edu, vhc2@psu.edu.

Received for review May 6, 2010 and accepted July 14, 2010.

Published online July 28, 2010. 10.1021/nn101289p

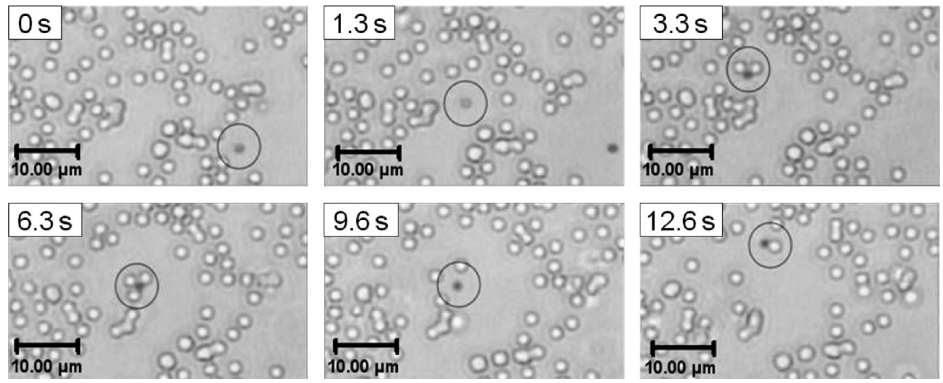

Figure 1. Optical microscope images of particle motions. A AgCl particle (dark particle, circled) mixed with 2.3 μm diameter silica tracers (light particles) in 1% (v/V) H_2O_2 under UV illumination. The AgCl particle alternates between attracting and binding to nearby silica particles for several seconds, then releasing them and engaging in a brief period of supra-Brownian diffusion before the next binding event. Supporting Information, Video 2 provides a representative sample of this behavior.

substrate for several seconds and then rapidly traversing several body lengths (~30 μm) in less than a second: a supra-Brownian, powered diffusion that abruptly terminates when the particle sticks again to the surface. This oscillatory particle motion is depicted in Supporting Information, Video 1. In this experiment, the spacing between AgCl particles is sufficiently large that interactions between them can be neglected.

When added to the system, 2.3 μm diameter silica tracer spheres provide an alternative (and preferred) target for AgCl particle attachment. Hence, the AgCl particles now attract, bind to, and then abruptly release the silica tracers. The cycle then repeats, with each cycle taking place over the course of a few seconds, as depicted in Figure 1 and Supporting Information, Video 2. These oscillatory binding events repeat over many cycles—125 cycles over 15 min—with no change in external stimuli. When the UV light is removed or the H_2O_2 is depleted, the oscillations cease, but they can be reinitiated with the addition of fresh H_2O_2 or reillumination.

This system is similar in composition to one previously reported by our group,[24] but with one crucial addition: H_2O_2. Also, in the previous system without H_2O_2, the direction of tracer particle pumping was constant and could be changed only by changing the wavelength of the illuminating light or the type of tracer particle used. That the H_2O_2 chemical fuel plays a critical role in creating spontaneous oscillations is not surprising, since complex nonlinear behavior in chemical systems only occurs if the systems are open (*i.e.*, nonequilibrium).

Mechanism for Oscillatory Behavior. When silver chloride is exposed to UV light in water in the absence of H_2O_2, it decomposes through a multistep pathway that yields the following net reaction:[25]

$$4AgCl + 2H_2O \rightarrow 4Ag + 4H^+ + 4Cl^- + O_2 \quad (1)$$

In deionized water, the resulting protons and chloride ions induce motion of the AgCl particles through diffusiophoresis.[24,26] In this mechanism, the more rapid diffusion of H^+ ($D = 9.311 \times 10^{-5}$ cm^2 s^{-1}) relative to Cl^- ($D = 2.032 \times 10^{-5}$ cm^2 s^{-1})[27] yields an inwardly directed radial electric field around the particle. The asymmetrical shape of the AgCl particle[24] produces imbalances in the angular distributions of the Cl^- and H^+ ions around the particle, yielding a net electric field at the particle surface, to which the particle itself responds. Nearby tracer particles also respond to this diffusiophoretic electric field, as governed by their zeta potentials. For particles with relatively thin double layers in low-Reynolds-number fluids, as is the case for this system, the speed at which the particle travels in response to a given ion gradient has been shown to be size independent.[26] Thus, although these experiments were performed starting with micrometer-sized particles for ease of imaging, the same propulsive mechanism holds true for much smaller particles.

The silver metal byproduct, which plates out onto the surface of the particle, plays a dual role: it creates additional color centers, thereby increasing the amount of light absorbed by the AgCl and making the reaction autocatalytic, but it also covers the AgCl surface and thus impedes the reaction.[24,25] The detailed morphology (see Supporting Information) of the Ag overlayer likely determines which of these effects dominates: small patches of Ag with a large edge/area ratio likely favor autocatalysis, but large patches of Ag will simply obscure the particle. Although oxygen bubbles occasionally issue from regions of particularly high AgCl/Ag particle density when the H_2O_2 concentration is high (above ~2% (v/V)), few or no bubbles occur for lower H_2O_2 concentrations and less dense particle distributions, thus facilitating analysis.

In addition to this decomposition pathway, silver metal is known to oxidize in the presence of H_2O_2.[28,29] In the presence of protons and chloride ions, such as those produced by eq 1, silver metal can be converted back into AgCl:

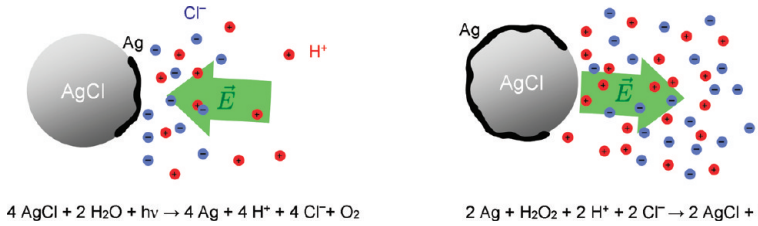

Figure 2. A schematic depiction of diffusiophoresis. Diffusiophoresis occurs due to the differing diffusivities of positive (H^+) and negative (Cl^-) ions produced or consumed at the particle surface. For simplicity, the ion distributions are shown only on one side of the particle.

$$2Ag + H_2O_2 + 2H^+ + 2Cl^- \rightarrow 2AgCl + 2H_2O \quad (2)$$

These two countervailing reactions—one which decomposes AgCl and the other which regenerates it—appear to give rise to the oscillatory motion observed, a motion which is driven by the free energy of the UV photons and the net decomposition of H_2O_2 into oxygen gas and water. Most oscillatory chemical systems consist of complex reaction networks with multiple intermediate species and negative feedback, usually with competing positive feedback.[30] The precise sequence of intermediate reactions implicit in eqs 1 and 2 is not known at this point, although they likely mirror those of the Bray−Liebhafsky oscillating reaction.[31]

When the reaction of eq 1 predominates, the particle is a net source of protons and chloride ions, and the higher diffusivity of protons yields a net electric field pointing toward the particle. Conversely, under the reaction of eq 2 the particle is a net sink of these ions, and higher diffusivity of protons implies a more pronounced depletion of Cl^- than H^+ near the particle surface, hence the electric field points away from the particle (Figure 2). A particle whose surface alternates between these two net reactions would thereby produce an oscillating electric field in solution, which would induce a concomitant oscillation in the motion of nearby tracer particles. During the tracer-attracting phase, one anticipates binding between a positive particle and negative tracer (further facilitated by the attractive van der Waals component of the interaction).

Oscillation of Silver/Silver Chloride Hybrid Particles. If the system described by the above equations is indeed oscillatory, then it should be possible to initiate the oscillations by starting with the reactants of eq 2 rather than those of eq 1. This is indeed the case: Silver particles in a solution of H_2O_2 (0.83% (v/V)) containing chloride ions (333 μM) and silica tracers cyclically attract and repel the tracers when illuminated with UV light in much the same way as does the AgCl system, as shown in Supporting Information, Video 3. Field emission scanning electron microscopy (FE-SEM) indicates that initially smooth, uncapped, single-crystal silver particles develop roughened growths of AgCl after exposure to H_2O_2 and chloride ions (Figure 3), the identity of which was confirmed by Auger spectroscopy (Supporting Information).

Although the most controlled method of initiating the oscillatory reactions is to begin with either pure AgCl or these single-crystal silver particles, we have found empirically that hybrid Ag/AgCl particles produce the most striking collective behavior. These hybrid particles are prepared by simply exposing aqueous suspensions of AgCl particles to UV light in the absence of H_2O_2 for 25 min, so that eq 1 goes to completion on the surface of the particles. H_2O_2 is then added to obtain a 1% (v/V) H_2O_2 concentration, without removing the chloride-ion-rich supernatant. As shown in Supporting Information, Video 4, the result-

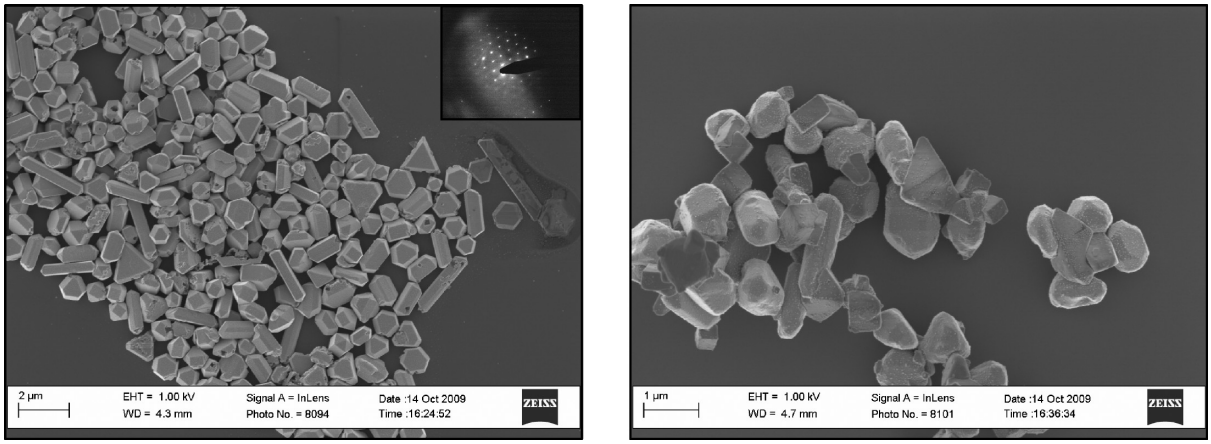

Figure 3. FE-SEM images and electron diffraction patterns of silver particles. (Left) Single-crystal silver particles with electron diffraction pattern (inset). (Right) Silver particles after exposure to 1% (v/V) H_2O_2, 30 mM HCl, and UV light for 15 min.

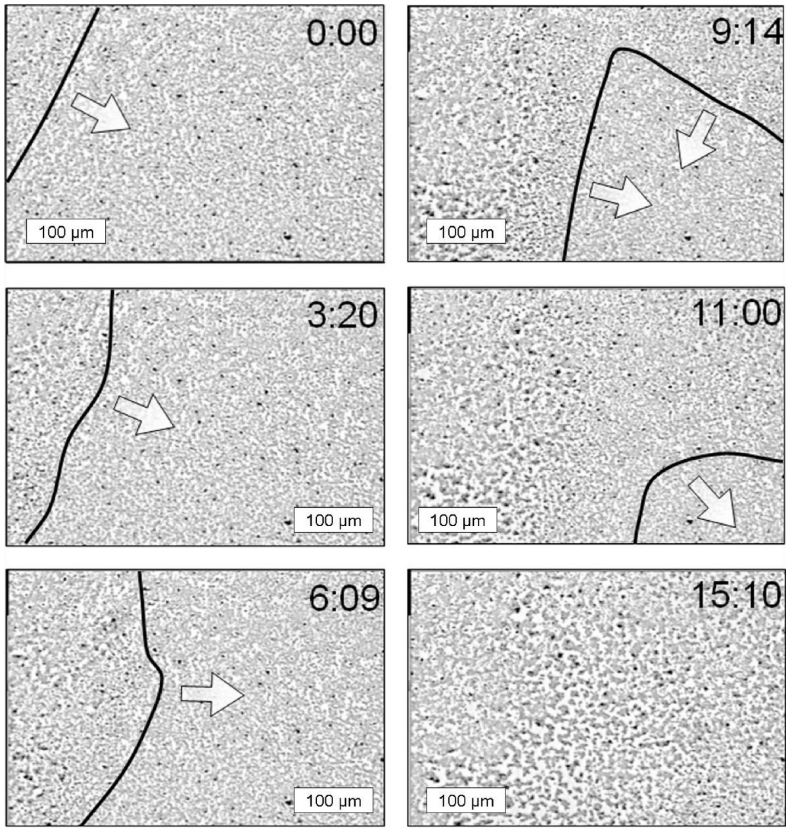

Figure 4. Optical microscope images showing the passage of a reaction front. A reaction wave moves in from the upper left and is joined by a second wave from the upper right. Solid lines trace the reaction front, defined as the line of maximum particle motion perpendicular to the front. After the front passes, the tracer particles are clumped. Since the video frame rate is 30 per sec, the time is given in the notation seconds:thirtieths.

ing system exhibits a rich variety of collective phenomena, including reaction waves, reversible clumping, and synchronized particle/tracer oscillations.

In the system described above, the catalyst particles exhibit roughening and eventual fragmentation into smaller nanoparticles. As noted above in the discussion of diffusiophoretic motion, the alternate growth and dissolution of silver metal is not homogeneous across the particle surfaces[24]—the AgCl particles become progressively more irregularly shaped and tend to break apart over time. This fragmentation increases both the number density of AgCl/Ag particles and their aggregate surface area, thus facilitating interparticle reaction synchronization and the propagation of chemical fronts, as described below.[3,32,33]

Emergent Behavior of Oscillating Particles. Open nonlinear chemical systems produce certain hallmark behaviors, as defined by the linear stability of the system in the vicinity of reaction fixed points and the larger topology of trajectories that interconnect fixed points. The simplest form of nonlinear behavior is bistability: the system has two distinct states, each persistently stable. A transition between two such states can propagate across a system as a step-like reaction wave. Figure 4 and Supporting Information Video 5 depict such a wave in our system. The system initially is largely uniform, with the darker Ag/AgCl particles having repelled the silica tracers. A reaction wave moves through the system from the upper left, later merging with a similar wave from the upper right. After the wave's passage, the silica tracers are clearly clumped around the darker Ag/AgCl particles indicating that the passing reaction wave is associated with a transition from a Ag-dominated state toward a AgCl-dominated state. In this way, reactions occurring within the thin, nanometer-scale surface layers of individual particles collectively combine to initiate changes in the system that propagate on the millimeter scale.

As a suitable reaction parameter is continuously varied, the qualitative dynamics of a nonlinear system (such as a chemical oscillator) can abruptly change when the linear stability of the fixed point changes in a so-called bifurcation. For example, stable limit-cycle oscillations can begin when a complex−conjugate pair of eigenvalues at a fixed point acquires a positive real part.[34,35] In a spatially extended system, the phases of local oscillators are diffusively coupled, leading to, for example, synchronization.[36] Such synchronization of distinct oscillating clusters of particles can be seen in Supporting Information, Video 4. Particles that belong to the same cluster are very strongly coupled and oscillate in synchrony as a single supereroscillator, wherein the diffusiophoretic fields of all the particles overlap into a synchronized communal field. Clusters form when local inhomogeneities in par-

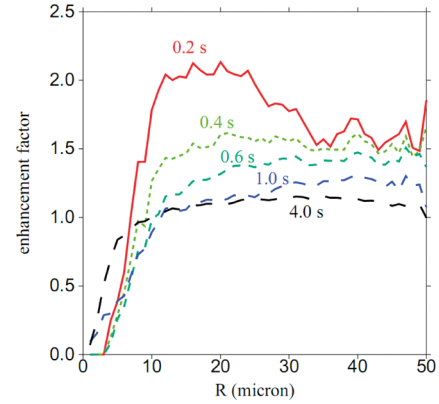

Figure 5. Calculated enhancement in the rate of cluster explosions. The local enhancement is calculated from the rate at which particle clusters within a distance *R* and time period $\pm\Delta t$ (colored lines) of a given explosion initiate an explosion of their own. The rate is normalized to the average local rate of cluster explosions, so that values above one correspond to a higher-than-average number of explosions per unit time within that disk of radius *R*, with an enhancement factor of 2 corresponding to a doubling of the rate (see eq. 3).

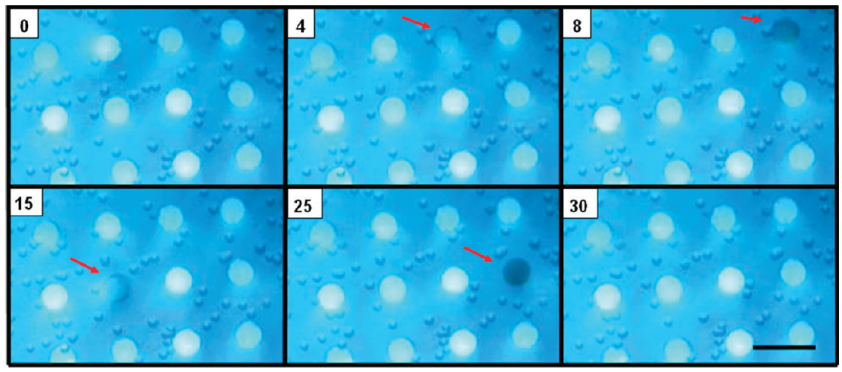

Figure 6. Optical microscope images of silver discs during the passage of a reaction front. Silver disks patterned on a SiO_2 wafer, in the presence of 0.17% (v/V) H_2O_2, 0.33 mM HCl, and silica tracer spheres. The surface is illuminated with UV light. Over the course of one second, a front of chemically induced tracer particle motion passes over the silver features, and their color alternates between reflective and dark. Red arrows indicate darkened features. The scale bar is 20 μm. Frame number is given in the upper left, captured at 30 frames per second.

ticle density favor the collapse of higher-than-average-density regions through the overlap of radial diffusiophoretic fields on nearby particles, and the size scale of these clusters is limited by the distance that a superdiffusing particle travels in roughly one-half-period of the oscillation.

Quantification of Emergent Behavior. Adjacent clusters of particles show a more subtle coupling that can be revealed by a statistical analysis. The most precisely defined moment in a cluster oscillation is the explosion: the abrupt initiation of a rapid cluster expansion as the radial diffusiophoretic field changes sign. The time and location of each such cluster explosion across a 11 s time span within a 150 × 106 μm field at the lower left of Supporting Information Video 4 were recorded, 124 explosions in all. For each explosion, the rate at which *other* explosions occurred within a radius R and time period $\pm\Delta t$ was recorded. These nearby-explosion-influenced rates were averaged over all the explosions and normalized by the average rate at which clusters exploded within the given radii regardless of the time that they occurred (eq 3). Only those explosions whose cylinders (defined by: R, $\pm\Delta t$) fell completely within the video clip were included in this analysis. Figure 5 depicts the computed rate enhancements associated with clusters having nearby neighbors which have exploded recently. The dip near $R = 0$ demonstrates that a second explosion is highly unlikely to occur immediately after a previous explosion at the same location; this is to be expected, since a given cluster has a refractory period between explosions. More interesting is the pronounced peak near 20 μm, especially strong for the shortest time delays. This peak is clear evidence of synchronization between cluster explosions: the probability that a given cluster will explode doubles if another cluster has just exploded nearby. Nearby clusters apparently couple through the diffusion of ions and/or the propagation of reaction waves. At the longest delay times, the enhancement factor approaches the asymptotic value of 1, as expected.

What generates these repeated cluster explosions and coalescences? Individual clusters may be on genuine attractive limit cycles;[34,35] alternatively, the collapsed state may represent a fixed point from which clusters are repeatedly disturbed *via* intercluster interactions until they are finally kicked into the basin of attraction

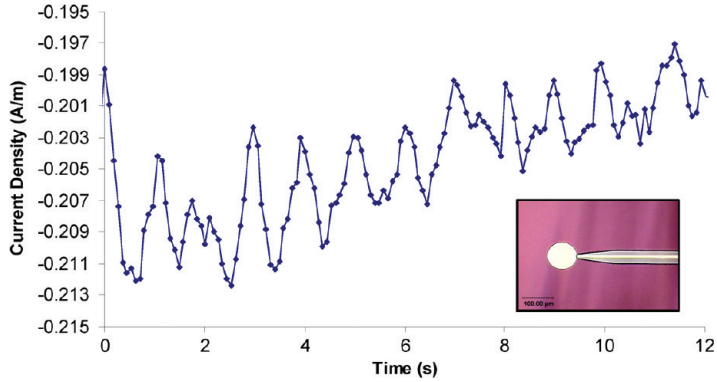

Figure 7. Current from a 90 μm silver disk patterned on a SiO_2 wafer in the presence of 0.17% (v/V) H_2O_2, 0.17 mM HCl, and silica tracer spheres, under UV illumination. After a few seconds of illumination, current oscillations are recorded which match the oscillations of tracer particles (Supporting Information, Video 8). Negative currents are oxidative with respect to the silver surface. Inset: the 90 μm diameter silver disk connected to an insulated silver wire that monitored the reaction current on the disk surface.

of a dispersed steady state.[34,35] Even in this second case, the reaction parameters are probably close to values that support a genuine limit cycle.

$$\text{rate enhancement} = \frac{\sum_{i=1}^{*} \text{rate of explosions within } (R, \pm\Delta t), \text{ exclusive of } i}{\sum_{i=1}^{*} \text{rate of all events occuring within } (R) \text{ of explosion } i, \text{ inclusive of } i} \quad (3)$$

Oscillations Using Fixed Silver Surfaces. Since the oscillations can be initiated with silver nanoparticles in the appropriate solutions, we also examined this system with silver disks lithographically patterned onto SiO_2 wafers to gain better control over the location, size, and surface properties of the catalytic surfaces. When isolated silver disks 50 μm in diameter are exposed to a solution of H_2O_2 and HCl under UV light, silica tracer particles near the edges of the disks oscillate alternately toward and away from the silver disk. Over time the initially reflective silver surface blackens, indicating the buildup of AgCl, as shown in Supporting Information, Video 6.

Similar to Figure 4, waves of tracer particle motion associated with the passage of chemical fronts can be seen when these lithographically patterned silver disks are arranged into arrays. A particularly remarkable effect was observed with arrays of the smallest disks studied, 9 μm in diameter at a 20 μm center-to-center spacing. When such a front propagated across this smallest silver disk array, the color of individual disks switched from reflective silver to dark AgCl and then back to reflective silver within a few tenths of a second, as shown in Figure 6 and Supporting Information Video 7.

In a modified version of the surface described above, a conductive silver wire was connected to a 90 μm diameter silver disk. This wire was then covered with insulating SU-8 polymer photoresist to isolate it from the solution and connected through an ammeter to a gold counter-electrode. As shown in Figure 7 and Supporting Information Video 8, the resulting current shows periodic variations, which correspond to the oscillatory motions of the tracer particles around the disk. While eqs 1 and 2 suggest that the current should alternate between positive and negative values, the negative offset of the current profile suggests that the oxidative reaction dominates, which is consistent with the observed darkening of the surface over time, that is, AgCl builds up.

CONCLUSIONS

We have described a new oscillating reaction that generates collective, organized powered motions within populations of chemically active nanoparticles. The rich set of particle behaviors observed is clearly electrochemical and diffusiophoretic in origin: oscillatory particle motion can be initiated with two distinct yet related sets of reactants and there are strong correlations between electrical current, surface color, surface charge, and particle motion. Positive feedback can amplify local variations in nanoparticle density to form tight particle clusters; these clusters then engage in correlated, collective behavior. Although further study is needed to fully elucidate the detailed mechanism of this oscillation, it likely involves the reactions depicted in eqs 1 and 2. It has been suggested that oscillatory reactions on the surfaces of self-propelled microscopic swimmers could induce "intelligent" collective behavior;[37] this is the first reported example of such a system. Further, the observation of reversible diffusiophoretic particle motion could be useful in the search for other oscillatory systems.

MATERIALS AND METHODS

AgCl particles were synthesized by a method similar to the one reported previously by our group.[24] Briefly, a trace amount (0.15 g) of sodium polyphosphate (85%, Aldrich) was added to a 100 mL solution of 0.4 M KCl (ACS grade, EMD) in deionized water, and the solution was heated to 70 °C. Under vigorous stirring, this solution was added to a second solution of 50 mL which contained 0.8 M $AgNO_3$ (99.995%, Alfa Aesar) and which was also at 70 °C. The reaction flask was covered with aluminum foil, and stirring was halted after 1 min. The resulting mixture was kept at 70 °C for 3 h followed by 100 °C for 1 h. The resulting white AgCl particles were then centrifuged down and redispersed into deionized water. This washing with deionized water was repeated several times. Large aggregates of AgCl were removed by centrifuging the suspended AgCl particles at 2000 rpm for 2 min and collecting the supernatant. If large aggregates persisted, this process was repeated on the supernatant, itself.

Uncapped single crystal silver nanoparticles were made simply by placing a short section (~0.05 g) of silver wire (99.99% pure, 1.5 mm diameter, Kurt J. Lesker Co.) into 15 mL of 30% H_2O_2 (VWR) in a scintillation vial at room temperature. The reaction was then allowed to go to completion. WARNING: this reaction is very exothermic, auto accelerating, and evolves a significant amount of gas. The initially room temperature solution reaches 100 °C within approximately 20 min without any external heat source. Silver nanoparticles are then centrifuged out of the supernatant after gas evolution has ceased.

Patterned wafer surfaces were made by standard contact lithography. Briefly, a silicon wafer (Silicon Quest, [100], p-doped, boron) with a 250 nm thermally grown oxide was use as a substrate. This same type of wafer was used as a substrate for the Auger measurements. Liftoff resist LOR-5A (Microchem) was spun on dynamically at 3000 rpm for 1 min, followed by a soft-bake at 170 °C for 1 min. The positive photoresist Megaposit SPR 3012 (Dow) was then spun on dynamically at 4000 rpm for 1 min followed by a soft-bake at 115 °C for 1 min. The wafers were exposed for 6 s, and then hard-baked for 1 min at 115 °C. Wafers were developed in Microposit MF CD-26 developer (Shipley) for 90 s. Wafers were washed thoroughly in deionized water and cleaned in an O_2 plasma. Silver metal was evaporated onto the surface with an e-beam evaporator at a rate of 1−2 Å/s. Liftoff of the sacrificial metal and photoresist was done in acetone and CD-26 baths. The wafers were then washed several times with deionized water. For patterns requiring the polymer insulator, Su8-2 was spun on at 2000 rpm for 1 min, soft baked in three stages at 65, 95, and 65 °C for one min each, exposed for 30 s, hard baked in three stages at 65, 95, and 65 °C for one min

each, and then developed in Su8 developer (Microchem). Wafers were washed with deionized water and isopropyl alcohol.

In a typical experiment a 9 mm diameter, 0.12 mm thick Secure-Seal imaging spacer (Sigma-Aldrich, cat. no. S7935) was placed on a microscope slide (VWR, cat. no. 48300-025), and the appropriate solutions were added. Except for experiments involving the patterned silicon wafers, no cover slide was used. For current measurements, two imaging spacers were overlaid on one another with a 0.1 mm diameter gold wire (99.99%, Aldrich) lying in between them, spanning the entire chamber diameter. The wire lay nearly, (so as to not block the light from the microscope objective) above the illuminated Ag feature to act as a counter electrode. The entire assembly was covered with a glass coverslip.

Acknowledgment. The authors thank T. Mallouk for his valuable insights and M. Dirmyer for XPS and the electron diffraction spectra. This research was supported by the Pennsylvania State University Materials Research Institute Nano Fabrication Network and the National Science Foundation Cooperative Agreement No. 0335765—the National Nanotechnology Infrastructure Network, with Cornell University. Additional funding from the National Science Foundation came from the Center for Nanoscale Science (NSF-MRSEC, DMR-0820404).

Supporting Information Available: Eight videos depicting the oscillatory behavior described in the text, and one pdf file containing Auger and XPS spectra, particle FESEMs, and video captions. This material is available free of charge *via* the Internet at http://pubs.acs.org.

REFERENCES AND NOTES

1. Fechner, A. Ueber Umkehrungen der Polarität der Einfachen Kette (On the Reversals of Polarity of a Simple Chain Reaction). *Schweigg J.* **1828**, *53*, 61–77.
2. Imbihl, R.; Ertl, G. Oscillatory Kinetics in Heterogeneous Catalysis. *Chem. Rev.* **1995**, *95*, 697–733.
3. Vanag, V.; Epstein, I. Localized Patterns in Reaction−Diffusion Systems. *Chaos* **2007**, *17*, 037110.
4. Mikhailov, A.; Showalter, K. Introduction to Focus Issue: Design and Control of Self-Organization in Distributed Active Systems. *Chaos* **2008**, *18*, 026101.
5. Miguez, D.; Muñuzuri, A. On the Orientation of Stripes in Fish Skin Patterning. *Biophys. Chem.* **2006**, *124*, 161–167.
6. Suzuki, N.; Hirata, M.; Kondo, S. Traveling Stripes on the Skin of a Mutant Mouse. *Proc. Nat. Acad. Sci.U.S.A.* **2003**, *100*, 9680–9685.
7. Wang, X.; Gruenstein, E. Mechanism of Synchronized Ca^{2+} Oscillations in Cortical Neurons. *Brain Res.* **1997**, *767*, 239–249.
8. Coullet, P.; Toniolo, C.; Tresser, C. How Much Information Can One Store in a Nonequilibrium Medium. *Chaos* **2004**, *14*, 839–844.
9. Belousov, B. P. A Periodic Reaction and its Mechanism. *Collection of Short Papers on Radiation Medicine*; Medzig: Moscow, 1959; p 145−152.
10. Zhabotinsky, A. Periodic Oxidation Reactions in the Liquid Phase (in Russian). *Proc. Acad. Sci. USSR* **1964**, *157*, 392–395.
11. Zaikin, A.; Zhabotinsky, A. Concentration Wave Propagation in Two-Dimensional Liquid-Phase Self-Oscillating System. *Nature* **1970**, *225*, 535–537.
12. Toiya, M.; González-Ochoa, H.; Vanag, V.; Fraden, S.; Epstein, I. Synchronization of Chemical Micro-Oscillators. *J. Phys. Chem. Lett.* **2010**, *1*, 1241–1246.
13. Yoshida, R.; Yamaguchi, T.; Kokufuta, E. New Intelligent Polymer Gels: A Self-Oscillating Gel with Pacemaking and Actuating Functions. *J. Artif. Organs* **1999**, *2*, 135–140.
14. Yashin, V.; Balazs, A. Pattern Formation and Shape Changes in Self-Oscillating Polymer Gels. *Science* **2006**, *314*, 798–801.
15. Sakai, T.; Yoshida, R. Self-Oscillating Nanogel Particles. *Langmuir* **2004**, *20*, 1036–1038.
16. Yoshikawa, K.; Aihara, R.; Agladze, K. Size-Dependent Belousov−Zhabotinsky Oscillation in Small Beads. *J. Phys. Chem. A* **1998**, *102*, 7649–7652.
17. Tinsley, M.; Taylor, A.; Huang, Z.; Wang, F.; Showalter, K. Dynamical Quorum Sensing and Synchronization in Collections of Excitable and Oscillatory Catalytic Particles. *Phys. D* **2010**, *239*, 785–790.
18. Sánchez, S.; Pumera, M. Nanorobots: The Ultimate Wireless Self-Propelled Sensing and Actuating Devices. *Chem. Asian J.* **2009**, *4*, 1402–1410.
19. Wang, J. Can Man-Made Nanomachines Compete with Nature Biomotors. *ACS Nano* **2009**, *3*, 4–9.
20. Mirkovic, T.; Zacharia, N.; Scholes, G. D.; Ozin, G. A. Nanolocomotion—Catalytic Nanomotors and Nanorotors. *Small* **2010**, *6*, 159–167.
21. Paxton, W.; Sundararajan, S.; Mallouk, T.; Sen, A. Chemical Locomotion. *Angew. Chem., Int. Ed.* **2006**, *45*, 5420–5429.
22. Sen, A.; Ibele, M.; Hong, Y.; Velegol, D. Chemo and Phototactic Nano/Microbots. *Faraday Discuss.* **2009**, *143*, 15–27.
23. Hong, Y.; Velegol, D.; Chaturvedi, N.; Sen, A. Biomimetic Behavior of Synthetic Particles: From Microscopic Randomness to Macroscopic Control. *Phys. Chem. Chem. Phys.* **2010**, *12*, 1423–1435.
24. Ibele, M.; Mallouk, T.; Sen, A. Schooling Behavior of Light-Powered Autonomous Micromotors in Water. *Angew. Chem., Int. Ed.* **2009**, *48*, 3308–3312.
25. Calzaferri, G. At the Time He Made the First Photographs on Paper: Did Henry Fox Talbot Oxidize Water to Oxygen with Sunlight? *Catal. Today* **1997**, *39*, 145–157.
26. Anderson, J. Colloid Transport by Interfacial Forces. *Annu. Rev. Fluid Mech.* **1989**, *21*, 61–99.
27. Lide, D., Ed. *CRC Handbook of Chemistry and Physics*, 87th ed.; CRC Press/Taylor and Francis: Boca Raton, FL, 2006; pp 5−76.
28. Maggs, F.; Sutton, D. Some Aspects of the Catalytic Decomposition of Concentrated Hydrogen Peroxide by Silver. Part 1. The Solubility and Rate of Solution of Silver. *T. Faraday. Soc.* **1958**, *54*, 1861–1870.
29. Joksimović-Tjapkin, S.; Delić, D. Kinetics of Concentrated Hydrogen Peroxide Decomposition on a Rotating Disk. *Ind. Eng. Chem. Fundam.* **1973**, *12*, 33–39.
30. Luo, Y.; Epstein, I. Systematic Design of Chemical Oscillators: Feedback Analysis of Mechanisms for Chemical Oscillators. *Adv. Chem. Phys.* **1990**, *79*, 269–299.
31. Sharma, K.; Noyes, R. Oscillations in Chemical Systems. 13. A Detailed Molecular Mechanism for the Bray−Liebhafsky Reaction of Iodate and Hydrogen Peroxide. *J. Am. Chem. Soc.* **1976**, *98*, 4345–4361.
32. Taylor, A.; Tinsley, M.; Wang, F.; Huang, Z.; Showalter, K. Dynamical Quorum Sensing and Synchronization in Large Populations of Chemical Oscillators. *Science* **2009**, *323*, 614–617.
33. *Oscillations and Traveling Waves in Chemical Systems*; Field, R.; Burger, M., Eds.; John Wiley and Sons: New York, 1985.
34. Guckenheimer, J.; Holmes, P. J. *Nonlinear Oscillations, Dynamical Systems and Bifurcations of Vector Field.*; Springer: New York, 1983.
35. Strogatz, S. *Nonlinear Dynamics and Chaos*; Addison Wesley: Reading, MA, 1994.
36. Kuramoto, Y. *Chemical Oscillations, Waves, and Turbulence*; Springer-Verlag: New York, 1984.
37. Balazs, A.; Epstein, I. Emergent or Just Complex? *Science* **2009**, *325*, 1632–1634.